J. Physiol. (1983), **341**, *pp.* 309–324
with 1 plate and 6 text figures
Printed in Great Britain

THE STRUCTURAL CORRELATE OF THE RECEPTIVE FIELD CENTRE OF α GANGLION CELLS IN THE CAT RETINA

BY LEO PEICHL AND HEINZ WÄSSLE

From the Max-Planck-Institut für Hirnforschung, Deutschordenstrasse 46, D–6000 Frankfurt/M. 71, F.R.G.

(*Received 12 October 1982*)

SUMMARY

1. The correlation between the receptive field centre and the dendritic tree of individual brisk transient, or α, ganglion cells in the cat retina was investigated by a combination of physiological and anatomical techniques.

2. The sizes of receptive field centres of brisk transient (Y) cells were measured with a flickering spot of light. Contour maps and response (or sensitivity) profiles were measured at mesopic and scotopic backgrounds.

3. Recording positions on the retina and nearby blood vessels were back-projected onto the receptive field plots on the tangent screen.

4. After recording, whole mount preparations of the retinae were stained by a reduced silver method to stain all α cells together with their dendritic trees. By comparing the landmarks on the screen plot with those of the whole mount it was possible to identify the recorded cells in the preparations and to study their morphology.

5. The dendritic tree of an α cell determines the position, size and shape of its receptive field centre.

6. The mesopic receptive field centres were found to be a factor of $1{\cdot}4 \pm 0{\cdot}13$ larger than their respective dendritic fields.

7. It is suggested that the dendritic fields of presynaptic neurones (bipolar and amacrine cell processes) add to the ganglion cell dendritic tree to produce the larger centre summating area.

INTRODUCTION

Structurally, the processes of each ganglion cell occupy a territory, the dendritic field, on the retinal sheet. Functionally, by virtue of the ocular optics each ganglion cell has a patch of outside world to look at, the receptive field (Hartline, 1938). It is a long-standing problem whether the receptive field centre is congruent with the cell's dendritic tree (Kuffler, 1953; Gallego, 1965; Brown & Major, 1966; Dowling & Boycott, 1966; Creutzfeldt, Sakmann, Scheich & Korn, 1970; Levick, 1975). In the cat retina a considerable amount of information on the morphology and function of ganglion cells has been gathered in the past and attempts to answer that question were made by comparing bulk data from physiology and anatomy, i.e. correlating the average receptive field centre with the average dendritic tree (Gallego, 1965;

Brown & Major, 1966; Leicester & Stone, 1967; Cleland & Levick, 1974; Famiglietti & Kolb, 1976; Peichl & Wässle, 1979). Information on cell class and retinal position was incorporated in these correlations so far as it was known, but this still left a large scatter in the data and hence some uncertainty, even discord, in the conclusions. By and large, receptive field centre and dendritic field were found to be in the same size range.

Nelson, Famiglietti & Kolb (1978) intracellularly recorded and stained ganglion cells in the isolated cat eye cup, enabling a straightforward comparison of the functional and anatomical extent of individual cells. Due to the limitations of their methods, however, they were not able to map receptive fields in detail and the use of vertical sections did not permit definitive statements on the relation between dendritic and receptive fields.

For one class of ganglion cells in the cat retina, the α cells, we are now able to obtain the dendritic morphology of individual cells in silver-stained retinal whole mounts after extracellular recording of their functional properties *in vivo* (Peichl & Wässle, 1981). In the present study detailed measurements of the receptive field dimensions were taken and then compared with the dendritic fields of the same cells.

METHODS

Experiments each lasting 2–3 days were done on six cats of either sex (2·0–4·2 kg). Details of the preparation of the animals are given by Peichl & Wässle (1979). In addition to nitrous oxide ventilation, barbiturate (Nembutal) was given intravenously at a rate of 1·0–1·25 mg/kg.hr, thus maintaining a suitable level of anaesthesia (Hammond, 1978), which was checked from time to time on the e.e.g.

Experimental procedure

The experimental set-up and techniques for extracellular recordings from retinal ganglion cells and optical stimulation were the same as given by Peichl & Wässle (1979). Contact lenses of zero power and an artificial pupil of 4 mm diameter were used. The refraction of the eye was measured with an eye refractometer and corrected for the screen distance by spectacle lenses. Experiments were terminated as soon as the eye media became cloudy.

In the experiments described here only brisk transient (Y) cells were investigated. They were recorded in the 'raphé' region of the cat retina where the probability of recording from somata rather than from axons is higher. Peichl & Wässle (1981) describe in detail the protocol used to classify a unit as belonging to the brisk transient (Y) class, to plot its receptive field centre (r.f.c.) on the tangent screen and to back-project a reference system of retinal landmarks onto that screen for subsequent identification of the corresponding α cell.

Identification of individual cells

The principal steps in the analysis of a brisk transient (Y) cell are illustrated in Pl. 1*A–D*. For each recorded cell the fundus with the electrode *in situ* was photographed by means of a Zeiss fundus camera to document the recording site with respect to nearby blood vessels (Pl. 1*A*). The unit's receptive field centre was plotted on the tangent screen under mesopic conditions. Then the response profile of the receptive field was measured at mesopic and scotopic backgrounds. Directly after the measurements the electrode position and neighbouring blood vessels were back-projected onto the tangent screen with the aid of the cross hairs of the fundus camera. This excluded shifts between receptive field plot and landmark plot caused by eventual drift movements of the eye. The resulting screen plot (Pl. 1*B*) contained the outline of the receptive field centre (in this case of two neighbouring cells), the electrode tip positions during recording and the blood vessel system in the recording area. At the end of the experiment the eye was excised under deep anaesthesia and the

retina stained as a whole mount with reduced silver. This stains the total α cell population with their dendritic trees. The recording area could then be determined by means of the blood vessels that are also visible in the preparation. Pl. 1*C* is a micrograph of the stained whole mount showing the retinal area corresponding exactly to the frame in Pl. 1*A*.

The α cells in that region were classified as on- or off-α by means of their stratification level in the inner plexiform layer. Dendrites of off-α cells ramify in a stratum close to the inner nuclear layer, those of on-α cells in a stratum some 10 μm nearer to the ganglion cell bodies (Nelson *et al.* 1978; Peichl & Wässle, 1981). Pl. 1*D* is a line drawing of the recording area with all α-cell somata. The recorded cells were then identified by the matching procedure described by Peichl & Wässle (1981). Their dendritic trees are drawn in Pl. 1*D* for comparison with the receptive field centres of Pl. 1*C*.

Receptive field centre map

For practical reasons cells were sampled about 2–5 mm away from the central area. α-cell density at this eccentricity is low enough to allow unequivocal identification of a recorded unit but still provides a convenient encounter frequency for recording. In addition, dendritic staining is most reliable in that retinal area. Centre diameters of brisk transient cell receptive fields at that eccentricity are roughly 2° of visual angle. The white-light spot used to explore the receptive fields had a diameter of 40′ of arc and was flickered on and off at 512 msec intervals. This stimulus was used for on-centre and off-centre units. For the off-centre cells the reaction to light-off was taken as centre response. Mesopic conditions consisted of a background luminance of 3–10 cd/m^2 and light spots of 24–32 cd/m^2 (background + stimulus) measured for the individual experiments with a luminance meter (Minolta).

First the r.f.c. border was mapped by observing the unit's discharge on an audiomonitor (see Peichl & Wässle, 1979), and marked on the tangent screen. Then we determined a response profile (Rodieck & Stone, 1965) for the horizontal and the vertical axis of the r.f.c. by measuring the unit's response to a flickering spot positioned at various points along the axis (see Fig. 1). The distance between successive points usually was 20′ of arc, i.e. the spot radius. For one unit a full two-dimensional scan of the r.f.c. response was made, requiring some fifty stimulus positions.

At each position a peri-stimulus time histogram (p.s.t.h.) from thirty-two stimulus presentations was averaged. We used the peak discharge of the transient response component for the response profiles and all further evaluation. For some units we compared response profiles that were derived from peak discharge values with those derived from the mean discharge rate (i.e. the unit's integral response) and they both produced the same r.f.c. dimensions. We therefore felt justified in taking the readily accessible peak discharge value as being equivalent to the unit's response.

Measurements of scotopic receptive field centres were done at a state of dark adaptation where surround responses could no longer be elicited (Barlow, Fitzhugh & Kuffler, 1957). Adaptation times of at least 15 min were used to achieve that state (approximately -2 log cd/m^2), coming from mesopic conditions.

Influence of stimulus size

In all receptive field measurements, i.e. acoustic plots and sensitivity profiles, stimulus position was defined as the mid-point of the 40′ light spot. Stimuli that are only partly inside the receptive field centre may provide enough light flux to elicit a response, hence there is a *prima facie* case that the stimulus size used influences the measured (as opposed to the true) r.f.c. size. This technical problem is assessed by Peichl & Wässle (1979). For the purpose of the present paper we estimated for one cell the distortion that a 40′ light spot under bad imaging conditions would introduce in the measured ganglion cell response profile. We used Robson & Enroth-Cugell's (1978) data to calculate the light distribution (or 'shape') of the retinal image of our stimulus for a 4 mm pupil and an assumed defocusing of 3D. (This is an improbable worst-case assumption because we used correcting spectacle lenses in the experiments.) This retinal image was then transformed by the measured intensity *vs.* response function of the ganglion cell under consideration to obtain the stimulus image as 'seen' by the cell. The cell's measured response profile is a convolution of the true profile with this stimulus image, and a deconvolution was applied to determine the true response profile. It turned out that the stimulus spot slightly broadened the profile by 4–5 % in diameter. It follows that even in the worst case the light stimulus used introduces only a minor error and therefore we did not attempt any corrections.

Accuracy of the matching procedure

The accuracy of superposition of the screen plot and the histological map is limited by two factors. One is the precision of the back-projection procedure. The beam of the fundus camera produces a light spot with blurred edges on the screen, and the centre of this spot which corresponds to the retinal point of aim can only be determined with an accuracy of 10′ of visual angle (5 mm on the screen), i.e. 30–40 μm on the retina. The second factor is the angular distortion occurring in the retina during histological processing. The retinal hemisphere is spread out as a flat mount, and local differential shrinkage occurs during the mounting procedure. After the retina is stuck to the slide, only minimal shrinkage and distortion is possible in the subsequent staining procedure. Displacements due to histological factors amount to about 50 μm.

This accuracy is sufficient to identify individual α cells unequivocally because they have an average inter-cell distance of some 200 μm at the eccentricities used here (see Pl. 1*B* and *D*). It means however that the relative position of the dendritic tree and the receptive field of a cell can only be described with a tolerance of 80–100 μm.

Histology

For the staining of α cells we used the protocol of Boycott & Peichl (Appendix to Peichl & Wässle, 1981). The method is generally reliable but shows variations in the extent to which dendrites are stained. For this study we used only cells that we judged to be well stained. This judgement is based on the comparison with cells in optimally stained reduced silver preparations and in Golgi preparations. The Discussion deals with this problem in detail.

Identified α cells were drawn by means of a Carl Zeiss drawing apparatus using a $\times 40/1{\cdot}0$ oil immersion objective (Zeiss, Planapo). Dendrites were followed under $\times 100$ before drawing to determine their extent as completely as possible. The magnification of the physiological r.f.c. plot was then adjusted to that of the dendritic field drawing for superposition.

RESULTS

Receptive field centre dimensions

Receptive field centre measurements resulted in an acoustically mapped contour line (Peichl & Wässle, 1981), and a quantitative response profile of the centre mechanism usually along two axes of the receptive field. Fig. 1 demonstrates the relations between these measurements for the receptive field of an off-brisk transient (Y) cell. The stippled area represents the acoustic r.f.c. map and the p.s.t.h.s show that stimulus positions outside this area still elicit a clear centre response. The response of the surround mechanism, activated during light-on, and also present in the receptive field centre region, dominates the unit's response at these r.f.c. border positions and this may be the reason why the acoustic plot underestimates the true extent of the centre mechanism.

In the present study we used the acoustic plot only to determine the position and the shape of a unit's receptive field centre. The r.f.c. diameters were always taken from response profiles. Fig. 2*A–D* presents response profiles for four brisk transient (Y) cells under mesopic (open circles) and scotopic (filled circles) conditions. Part *A* of the Figure contains sample p.s.t.h.s to show how the unit's response changes with stimulus position in the receptive field and adaptation level.

The maintained discharge of each unit at the same background illumination was also measured, and only those responses that were at least two standard deviations above the mean maintained discharge rate (dotted horizontal lines) were taken as stimulus-driven responses. They defined the extent of the centre mechanism, i.e. the r.f.c. diameter. The maximal response is usually in the geometric centre of the r.f.c.;

in some units one observes a slight but significant deviation of this peak from the r.f.c. mid point.

Response profiles, and consequently the r.f.c. diameters, may vary with the adaptation level of the retina (Andrews & Hammond, 1970; Ahmed, 1981). For eight of the recorded units we measured the sensitivity profile also under scotopic

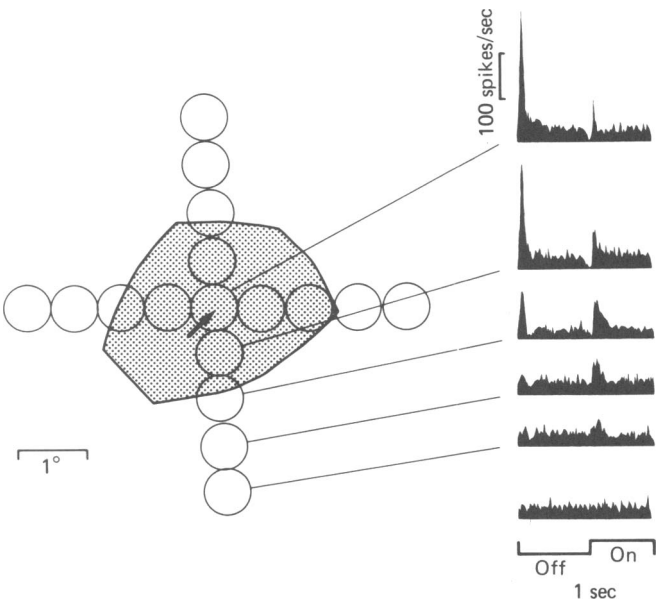

Fig. 1. Receptive field centre measurements of an off-brisk transient (Y) cell. The stippled area corresponds to stimulus positions, where a clear centre response could be detected on the audiomonitor. The circles represent stimulus size and positions for a horizontal and vertical scan through the receptive field, which were used to construct the response profiles. For each position p.s.t.h.s were averaged from thirty-two stimulus presentations. Some histograms from different parts of the receptive field are displayed on the right. The lowest p.s.t.h. shows the unit's maintained discharge when there is no stimulus. The arrow marks the back-projected electrode tip position during the recording. Same unit as Fig. 3, at 2·6 mm distance from the central area. Stimulus luminance: 30 cd/m² (stimulus + background); background luminance: 10 cd/m².

conditions, at background luminances of about -2 log cd/m², using stimulus intensities that elicited a discharge rate comparable to the mesopic situation. The units showed no surround response, and the scotopic response profiles (continuous lines with filled symbols in Fig. 2*A–D*) were always broader than the mesopic ones. Ratios of scotopic *vs.* mesopic r.f.c. diameters ranged from 1·2 to 2·8 (see Discussion).

Throughout the analysis of a unit we checked the positional stability of its r.f.c. on the screen by recurrent verification of the peak-response position, also before and after dark-adaptation times. Usually the mesopic and scotopic response profiles of a cell were concentric. Only in one case did we observe a shift between the mesopic and the scotopic peak response position (Fig. 2*B*).

The mesopic backgrounds used here (from 3 to 10 cd/m²) are in the mean to high

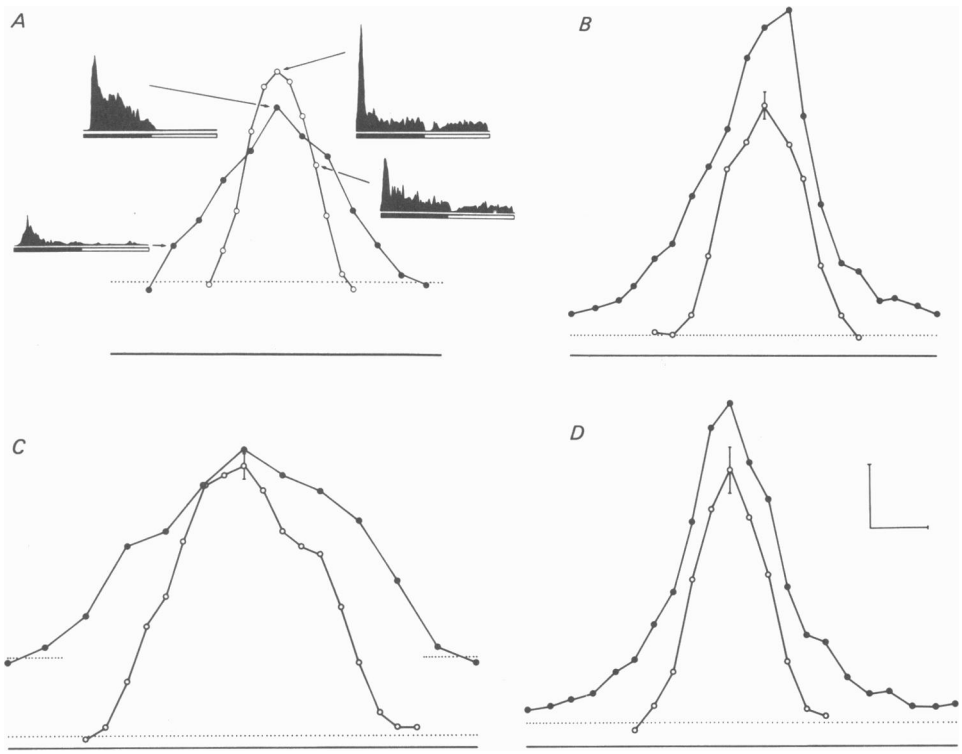

Fig. 2. Response profiles of the receptive field centres of four brisk transient cells plotted as a function of horizontal position in the receptive field. Open circles show responses under mesopic conditions (background 3·5 cd/m²), filled circles represent scotopic conditions (background approx. 0·01 cd/m²; stimulus + background approx. 0·02 cd/m²). In the profiles the ordinate is the peak discharge rate of the transient centre response as determined from the p.s.t.h.s. The S.D. (vertical bar) of the value for the maximal sensitivity position was determined by repeated measurements. The continuous lines indicate zero discharge, the dotted lines show the chosen significance level, two standard deviations above the mean maintained discharge. Scotopic and mesopic significance levels were similar in *A*, *B* and *D*, but differed in *C*. The stimulus spot of 40′ diameter was flickered on and off every 500 msec (1 Hz). *A*, off-centre cell from 4·4 mm eccentricity. Some p.s.t.h.s are inserted to show the differing histogram shape when comparing scotopic (histograms to the left) and mesopic (histograms to the right) responses. The scotopic histograms are more sustained and have a longer latency. *B*, on-centre cell from 2 mm eccentricity. Note the different position of the scotopic and mesopic sensitivity maximum. *C*, off-centre cell from 5·8 mm eccentricity. *D*, on-centre cell from 2·7 mm eccentricity. Mesopic stimuli (stimulus + background) had 32 cd/m² in *A* and *C*, and 24 cd/m² in *B* and *D*. The horizontal scale in *D* represents 1·5° for *A* and 1° for *B*, *C* and *D*; the vertical scale represents a discharge rate of 50 spikes/sec for *A* and *C* and of 100 spikes/sec for *B* and *D*.

mesopic range as stated by Andrews & Hammond (1970), and therefore our mesopic r.f.c. dimensions represent centre summation areas of mixed cone and rod input, but presumably cone-dominated. For technical reasons we could not use photopic conditions and thus not look into a possible further decrease of r.f.c. size for purely cone-mediated input.

Dendritic tree and receptive field centre

When a physiologically examined α cell was identified in the stained whole mount we judged (see page 319) its adequacy of staining and then drew the full dendritic tree, together with the surrounding blood vessels as landmarks. With the aid of these marks, which were also documented on the physiological r.f.c. screen plot, the two maps (anatomical and physiological) were brought to scale and superimposed. The

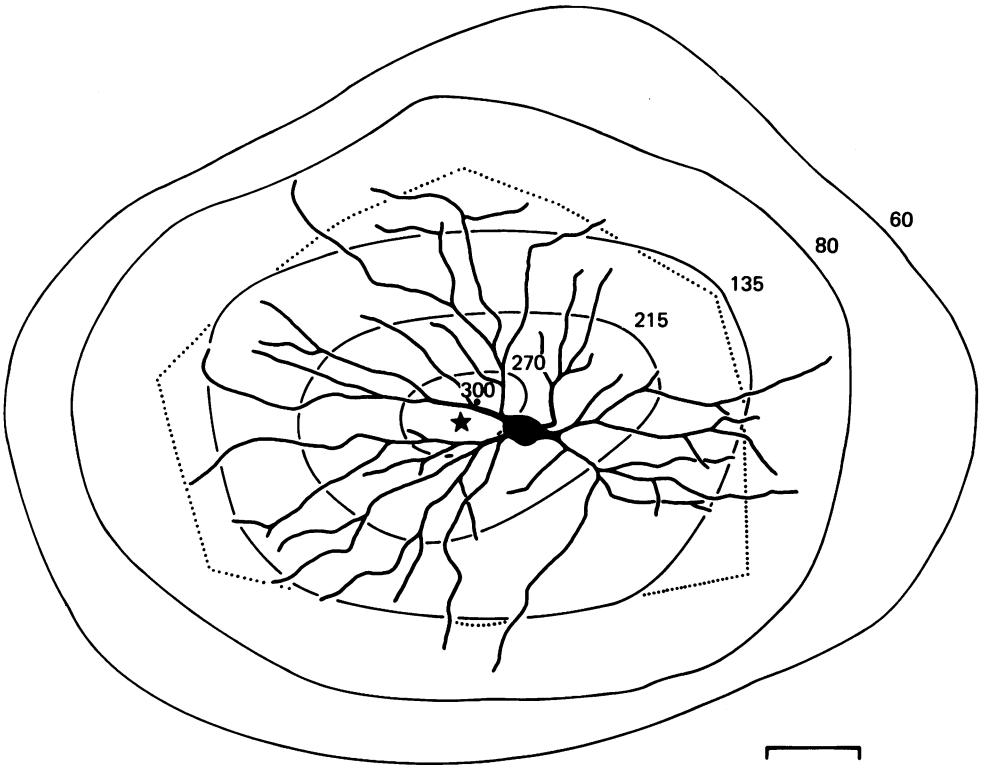

Fig. 3. Comparison of the dendritic tree and the receptive field centre of an off-brisk transient cell (same unit as Fig. 1). The continuous lines are equal response contours and represent peak discharges of 270, 215, 135, 80 and 60 spikes/sec. The maximum discharge of 300/sec is marked by the centre dot. The dotted outline indicates the border, where a clear centre response could be detected on the audiomonitor. The asterisk shows the electrode position. The scale bar represents 100 μm on the retina or 0·5° of visual angle.

optimal superposition still left slight mismatches (see Methods) so that in the following a tolerance of 80–100 μm in the relative position of dendritic tree and receptive field has to be accepted. In Figs. 3–5 we have centred the cell in the r.f.c. within that tolerance.

Fig. 3 shows the example of an off-α cell whose dendritic tree was recovered after a full two dimensional scan of its mesopic receptive field centre (same unit as Fig. 1; about 5 hr of recording). The dendritic tree represents the anatomical extent of this ganglion cell, hence the region in which it can make synaptic contact with input

neurones. The electrode-tip position, marked by an asterisk, shows that we recorded from near the soma.

The continuous, roughly elliptical lines are iso-response lines, i.e. lines of equal sensitivity constructed from the two-dimensional response profile. They range from a peak response of 300 spikes/sec to a response of 60 spikes/sec. The mean maintained activity of the unit was 32 ± 13 spikes/sec so that, according to the significance level defined above (two S.D. above maintained discharge rate), the 60 spikes/sec iso-response line represents the borderline of stimulus-driven activity. The acoustically determined r.f.c. outline is dotted. The shape of this outline is similar to the shape of the isosensitivity lines nearby; one can therefore accept the acoustic map as a faithful representation of the r.f.c. geometry. It approximates the size of the dendritic field, as did most of the acoustic r.f.c. plots in our earlier paper (Peichl & Wässle, 1981). The shape of the isosensitivity lines (and therefore the receptive field shape) approximates the shape of the cell's dendritic field.

For such an extensive r.f.c. plot the cell had to be recorded for several hours. In the following a simpler procedure is described, where the response profile is obtained quantitatively for two axes and the total shape is derived from the acoustic r.f.c. plot.

In Fig. 4 the physiological and anatomical features of another off-α cell are combined. This is the off-unit of Pl. 1, it was an axon recording some 100 μm away from the soma (recognized by damage to the axon which shows up as degeneration argyrophilia in the silver-stained whole mount). Fig. 4 *A* and *B* shows the horizontal and the vertical mesopic response profiles of this unit; they contain centre and surround responses. Note that the surround mechanism extends throughout the centre region. Details of the presentation are given in the Figure legend. In part *C* of the Figure the cell's dendritic tree and r.f.c. outline are superimposed, together with response p.s.t.h.s for three representative stimulus positions. In this and the following units the r.f.c. outline was obtained in the following way: comparison of the response profile diameter and the corresponding diameter in the acoustic r.f.c. plot gave a factor by which the acoustic plot had to be graphically enlarged. This corrected r.f.c. plot hence has the shape of the acoustic plot and the size of the sensitivity profile. In this unit again one obtains clear centre-responses outside the dendritic field region. The receptive field centre diameters are by a factor of 1·35 larger than the corresponding transsects through the dendritic field, resulting in an r.f.c. area 1·8 times larger than the dendritic field area. The shapes of the two, however, match closely: both have similar ellipticity and the same orientation of the long axis. Two more examples of the spatial relationship between dendritic field and receptive field centre of α cells are presented in Fig. 5. The r.f.c. extent was obtained in the same way as that in Fig. 4, the cells were superimposed according to the matching procedure outlined in Pl. 1. The hatched annulus indicates the size discrepancy between dendritic field and r.f.c. which is an areal factor of 1·5 in *A* and of 2·6 in *B*.

Altogether ten recorded cells in three retinae were adequately stained and analysed in this way. In all of them the position of the receptive field centre coincides with the dendritic field position on the retina, and the shapes of the two correspond closely. The size of the r.f.c. is substantially larger than the dendritic field size for all units (mean ratio 1·95, S.D. 0·35 in area; or 1·4, S.D. 0·13 in diameter; $n = 10$). On- and

off-cells do not differ significantly (area ratio for on-cells: mean 1·84, S.D. 0·34, $n = 5$; for off-cells: mean 2·06, S.D. 0·37, $n = 5$). For each brisk transient (Y) unit the receptive field centre has a peripheral zone (of 100–150 μm at the eccentricities investigated) where the cell is not anatomically present.

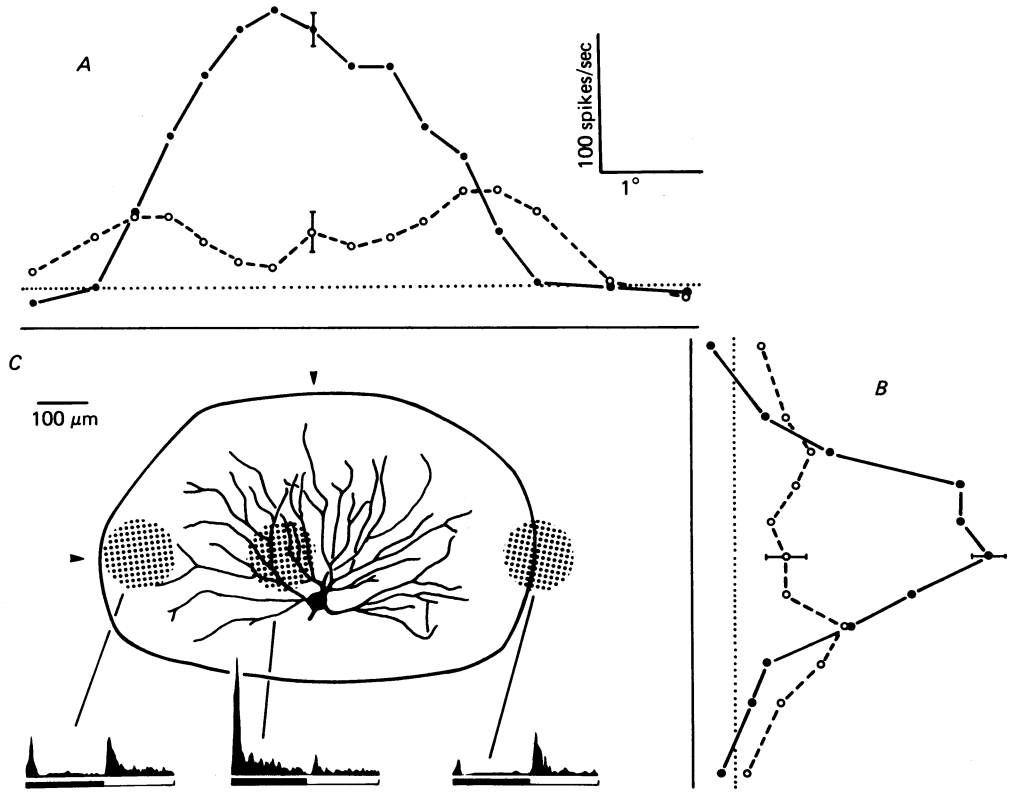

Fig. 4. Response profiles in relation to the dendritic tree of an off-centre brisk transient cell. *A* and *B* are horizontal and vertical response profiles. Filled circles show peak discharges at light off (centre response), open circles at light on (surround response). The surround response in the p.s.t.h.s, as can be seen in *C*, extends throughout the centre. The continuous straight lines show zero discharge, the dotted straight lines the significance level. In *C* the dendritic tree of the cell is drawn at the same scale as the response profiles. The two arrowheads indicate the intersects where the profiles were measured. Three selected positions of the light spot during the horizontal scan are indicated by stippled circles and the corresponding histograms are shown. The continuous outline in *C* is the enlarged acoustic plot described in the text. The unit was located at an eccentricity of 3 mm. Responses were to stimuli of 30 cd/m^2 (stimulus + background) at a background of 10 cd/m^2.

α cells in the cat retina often contain sectors or enclosed areas within their dendritic territory that are devoid of dendritic processes (see Figs. 3 and 5 and the illustrations of Peichl & Wässle, 1981 and Wässle, Peichl & Boycott, 1981). These dendrite-free regions may be 100 μm or more in size, but they do not show up as troughs in the response profiles.

Similarly we have never found a decreased response at r.f.c. positions that were in the shadow of the recording electrode. When recording from a ganglion cell body, the electrode shaft obscures a sector of the receptive field (see Pl. 1) but this is not noticed in the response profiles. Profiles of soma recordings show no characteristic difference from profiles of axon recordings, i.e. with an electrode position outside the receptive field.

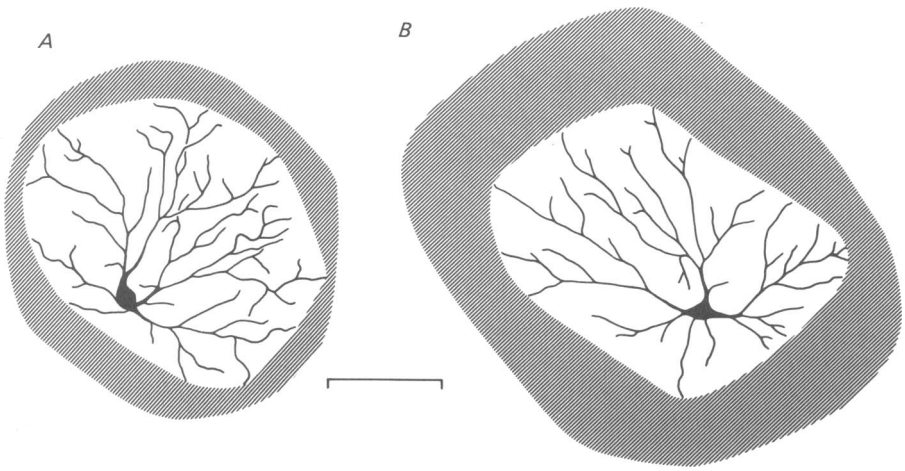

Fig. 5. Comparison of the receptive field centre and the dendritic field for two more cells. The hatched annulus indicates how much larger the receptive field centre is when compared with the dendritic field. *A*, on-centre cell from 4·4 mm eccentricity. *B*, on-centre cell from 4·8 mm eccentricity. *A* and *B* are from different experiments. The r.f.c.s were obtained under mesopic conditions. The scale is 200 μm for *A* and *B*.

DISCUSSION

For retinal ganglion cells one aspect of function has a very overt and direct relation to the neural morphology: a cell can only respond to light stimulation in that part of the retina where it has functional connexion with the photoreceptors (via interneurones, horizontal, bipolar and amacrine cells). Hence the dendritic field size determines the receptive field size, and from the match or mismatch between the two it should be possible to derive information about the spatial properties of the interneurones.

For concentrically organized receptive fields with centre–surround antagonism (Kuffler, 1953) the general claim was that the receptive field centre corresponded best to the area occupied by the dendritic field (Gallego, 1965; Brown & Major, 1966; Leicester & Stone, 1967; Cleland & Levick, 1974; Levick, 1975; Famiglietti & Kolb, 1976; Peichl & Wässle, 1979); surround sizes were so much larger that a correspondence between them was never seriously considered in mammals. Our aim in the present study was to determine the precision of congruence between the r.f.c. and dendritic field dimensions directly for the specifically identified retinal ganglion cell.

We used the α cells of the cat retina because they offered the possibility of obtaining the receptive field properties by stable extracellular recordings (for several hours in

the case of Fig. 3) and then recovery of the cell morphologically together with its dendritic tree (Peichl & Wässle, 1981).

The results show that the dendritic tree of an α cell determines the position, shape and size of its receptive field centre; however, the r.f.c. is nearly twice as large in area.

Before we deal with the interpretation and implications of these findings we have to consider some technical points bearing on the results. The correlations are based on receptive field centre and dendritic field measurements which, apart from measurement errors, involve definitions and assumptions.

Technical considerations

Receptive field centres

The receptive field centre is defined here as the region in which a centre response to light stimulation is clearly detectable above the maintained firing level in the p.s.t.h.s (see Methods). Receptive field centre size strongly depends on the method in use (acoustic plotting, area threshold or area response curves; for a discussion see Cleland & Levick, 1974 and Peichl & Wässle, 1979), and the r.f.c. diameters given here are about 50% larger than those derived from area threshold curves by Peichl & Wässle (1979). As pointed out in the Methods section, the stimulus size used and its optical degradation in the ocular media had only a minor influence on the measured r.f.c. size. Thus we regard the r.f.c. maps as an adequate representation of the centre summating region in shape and size, and an appropriate measure for comparison with the anatomy.

Our stimulus intensities were suprathreshold; therefore the mesopic centre measurements are surround-contaminated (see the histograms in Figs. 1 and 2*A*. Surround influence leads to a reduction in r.f.c. size and thus pure centre size may still be somewhat larger than given here. This would enhance the size difference between dendritic field and receptive field centre described in the Results.

The scotopic receptive field centres certainly represent purely rod-mediated centres, whereas the mesopic fields show the centre summation area of the cone mechanism with some rod influence and an additional surround contamination. Therefore the scotopic and mesopic centres as measured here should not be compared without caution and we abstain from giving detailed numerical values.

Our observations, however, are compatible with the more elaborate measurements and detailed results of Andrews & Hammond (1970) and Ahmed (1981), which showed that the majority of cells had larger scotopic than mesopic centres. In all our cells except one the scotopic and mesopic centres were concentric, thus fitting into Ahmed's B1 category.

Under scotopic conditions light stimuli were of a luminance that elicited responses similar to the mesopic ones, image degradation in the eye media was thus regarded as having an equally small effect on the response profiles.

Staining quality

Dendritic field dimensions are strongly dependent on the staining quality. Although our procedure reliably stains the total α cell population, the quality of dendritic staining varies from retina to retina and also across the retina. A detailed assessment of stainability problems is found in Wässle *et al.* (1981). Staining in any preparation is best along the raphé and we took our cells from there. Grossly understained preparations are readily recognizable and were not used for analysis, but also in an apparently well stained preparation there is the *prima facie* possibility of understaining. Very fine processes may not stain with neurofibrillar methods, probably due to a lack of resolvable filamentous protein, and should α cell dendrites end in finely tapered tips there would be a systematic underestimate of dendritic field dimensions.

Chance understaining of an individual cell can be detected by comparing its dendritic field area to that of the neighbouring cells. In reduced silver preparations there is only a limited size variance for neighbouring α cell dendritic trees. A typical example for a field of ten cells was a mean dendritic field diameter of 402 μm with a S.D. 37 μm (1·7 mm distance from the central area; see also Wässle *et al.* 1981). This is regarded as a true biological size variance and not a staining artifact, as neurofibrillar staining is non-capricious. Thus when an experimental dendritic field deviated more than approximately 10% from the mean size of its neighbours it was regarded as understained; when the deviation was less, it was regarded as an adequately stained individuum. With dendritic fields of 500–700 μm this judgement leaves a possible error of 50–70 μm in diameter.

A possible systematic understaining of experimental preparations was judged by comparing their mean dendritic field sizes to those of our best reduced silver preparations. Only preparations that passed this criterion were used here. In an earlier paper we have shown that the dendritic field dimensions of α cells in well stained reduced silver material are the same as those in Golgi-stained material corrected for shrinkage (Fig. 14 Wässle *et al.* 1981). However, as there is no means of knowing whether a cell is completely stained either with Golgi or with any other staining method, we can merely say that the dimensions of a well stained reduced silver cell are as close to reality as one can get for the time being.

Dendritic field *vs.* mesopic r.f.c. diameters as reported in the Results section show a mean difference of 40% (with a 10% S.D.; mean ratio r.f.c./dendritic field diameter $1{\cdot}4 \pm 0{\cdot}13$ S.D.; the smallest ratio was 1·2, the largest 1·6). Even in the worst case of a 5% over-estimate of the r.f.c. and a 10% underestimate of the dendritic field size one is faced with a difference of 20% between the anatomical and physiological extent of a cell. The scatter in the ratio given above may thus reflect varying staining quality of the cells, or it may be due to a genuine difference in convergence of presynaptic neurones.

Functional considerations

Dendritic tree and receptive field centre

Receptive fields are centred on their dendritic trees (within the tolerance of about 80 μm introduced by the method); there exists no lateral displacement between the two. This is in agreement with the fact that there are no obliquely running fibres in the cat outer retina comparable to the Henle fibres in the primate foveal region (well illustrated by Schultze, 1866) where such shifts occur. Thus the connexions between photoreceptors and ganglion cells through the retinal layers are essentially vertical in cat.

As Figs. 3–5 show, the receptive field centre of a representative α cell would consist of a central part of about 600 μm covered by dendrites and an annular region 100–150 μm broad where the cell is not anatomically present. It follows that there has to be a spatial convergence of interneurones onto the ganglion cell's dendritic field, thereby linking it to photoreceptors outside its dendritic territory.

Neurones presynaptic to the ganglion cells have their own dendritic and axonal fields over which they sum information and then convey it onto the ganglion cells. Fig. 6 is a diagram of the possible spatial relationships between these neurones. All data were taken from Golgi material to make dimensions consistent. (α cell: Boycott & Wässle, 1974, Wässle *et al.* 1981; bipolar cell dimensions: Boycott & Kolb, 1973; Famiglietti, 1981; Kolb, Nelson & Mariani, 1981.)

Similarly, areas within the dendritic field which are not covered by dendrites, and which may be about 100 μm wide, will not show up as points of decreased sensitivity in the response profiles as long as they are filled by the spread of the bipolar cells (illustrated by the central bipolar cell in Fig. 6), i.e. the input neurones have to smooth over such ganglion cell irregularities so as to produce a homogeneous sensitivity profile. This smoothing may also account for the fact that blood capillaries or a small electrode shaft within the r.f.c. are not showing up as dips in the response profiles.

Bipolars are not the only presynaptic elements to α ganglion cells. Kolb (1979) finds that α cells (her GI cells) get 80% of their input through amacrine synapses and only 20% by direct bipolar synapses. Within the range of 100–150 μm given by our experiments, the narrow field amacrine of Kolb *et al.* (1981) would be a candidate (see Fig. 6). The spatial properties of photoreceptors and horizontal cells (Nelson,

1977), as far as they concern the ganglion cell, must be incorporated in the receptive field properties of the bipolar cells, so they do not have to be treated as separate influences at the level of the inner plexiform layer.

In the dark-adapted retina the cone pathway: cone bipolar–(amacrine)–ganglion

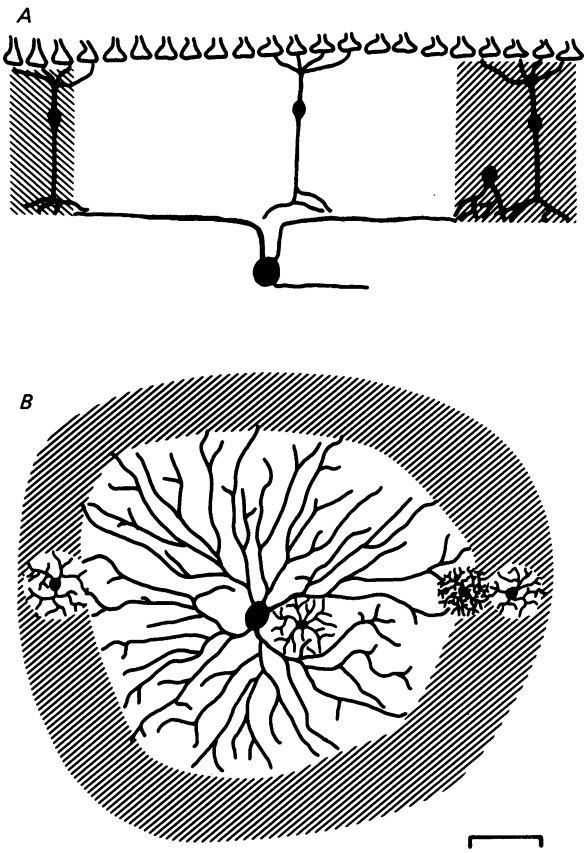

Fig. 6. Schematic drawing to explain the larger size of the receptive field centre when compared with the dendritic tree. *A* shows a vertical view of the retina, receptor pedicles on top and an α cell at the bottom. It can be seen how in the hatched parts the ganglion cell dendritic tree has access to photoreceptor information by the addition of bipolar and amacrine cell processes. *B* shows a plan view of the same arrangement. The hatched annulus indicates how the bipolar and amacrine cells enlarge the dendritic field. The bipolar cell inserted near the soma shows how sparse ganglion cell dendritic ramification can be bridged to make the sensitivity profile smooth. The scale bar in *B* is 100 μm and gives the approximate dimensions for cells of medium eccentricity as seen in Golgi preparations. *A* is not drawn to scale in the vertical direction.

cell is replaced by the scotopic pathway: rod–rod bipolar–rod amacrine–ganglion cell (Nelson, Kolb, Famiglietti & Gouras, 1976). For a substantial proportion of ganglion cells the scotopic r.f.c. is larger than the mesopic one (Ahmed, 1981, and possibly the units described here). This increased size discrepancy between r.f.c. and dendritic field must be due to the presynaptic neurones in the scotopic pathway. One has to assume

that at least some of them have a larger spread of processes and larger space constants than the interneurones operating in the mesopic state.

Nelson *et al.* (1978) report one α cell (their Fig. 5) with a receptive field centre smaller than the dendritic field. We never observed a similar case, and with the above considerations on the spatial extent of the presynaptic elements it is difficult to interpret such a relation. It may be that lack of the eye optics in their experiments produced a more variable measure of r.f.c. sizes.

In an earlier study we have compared r.f.c. sizes of brisk transient (Y) and brisk sustained (X) cells with dendritic field sizes of Golgi-stained α and β cells (Peichl & Wässle, 1979). For α cells we found a good match of r.f.c. and dendritic field sizes across the retina, with the r.f.c.s being slightly smaller. The difference between that and the present direct results is due to the use of a different r.f.c. measure (equivalent diameters derived from area threshold curves), giving smaller centre dimensions, and the use of bulk shrinkage factors. For the β cells we found a relation between r.f.c.s and dendritic fields which differed from that of α cells. A similar difference was stated by Cleland & Levick (1974). It would be intriguing to learn about this in individual β cells because, in contrast to α cells, β cells are found to have mainly bipolar input (70% bipolar, 30% amacrine synapses; Kolb, 1979).

Dendritic tree and sensitivity profile

Creutzfeldt *et al.* (1970) have suggested that the senstivity profile of a retinal ganglion cell is a product of its dendritic geometry and the biophysical properties of dendrites and synapses. They postulated that the sensitivity at any retinal point is proportional to the local dendritic density, weighted by the attenuation of the signal on its way to the soma due to dendritic cable properties. Thus a peripheral stimulus would be less effective because it stimulated fewer synapses (low dendritic density) and because the signal is attenuated more until it reaches the soma. Should a ganglion cell with an eccentrically located soma then have a skewed sensitivity profile with the maximum at the soma position?

The response profiles obtained in our experiments always had their maximum in the vicinity of the r.f.c. mid-point, even in those cases where histology revealed a very skewed dendritic tree. In the unit of Fig. 4 the maximal response occurs at a point in the dendritic field away from the soma and not morphologically conspicuous. Another example is the cell in Fig. 10 of Peichl & Wässle (1981) where the maximal sensitivity was also near the r.f.c. mid point. Our recordings were from the raphé region of the cat retina, where eccentric dendritic trees are very common for α cells (Wässle *et al.* 1981), so the general absence of skewed response profiles is a strong indication that there is no correspondence between soma and maximal response position as suggested by Creutzfeldt *et al.* (1970); the involved mechanisms seem to centre the response maximum at the dendritic field mid point.

Knowledge about the types of bipolars and amacrines presynaptic to any ganglion cell type and about their functional properties and interrelations has only recently begun to accumulate (for a review see Sterling, 1983), and more is necessary before one can draw the wiring diagram for a receptive field. An interesting perspective has been opened by the theoretical work of Koch, Poggio & Torre (1982), who have analysed the electrical properties of the α-cell dendritic tree. The simple question of

what causes the r.f.c. sensitivity profile may be answered soon by a combination of these two approaches – serial reconstruction of the synaptic inputs (Stevens, McGuire & Sterling, 1980) and mathematical analysis of their electrical properties (Koch *et al.* 1982).

We are grateful to B. B. Boycott, J. Bolz and D. I. Vaney for useful criticism throughout this study and on the manuscript, and to H. Ahmed, F. Boij, S. Hahn and I. Odenthal for technical and secretarial assistance.

REFERENCES

AHMED, B. (1981). The size and shape of rod and cone centres of cat retinal ganglion cells. *Exp. Brain Res.* **43**, 422–428.

ANDREWS, D. P. & HAMMOND, P. (1970). Suprathreshold spectral properties of single optic tract fibres in cat, under mesopic adaptation: cone–rod interaction. *J. Physiol.* **209**, 83–103.

BARLOW, H. B., FITZHUGH, R. & KUFFLER, S. W. (1957). Change of organization in the receptive fields of the cat's retina during dark adaptation. *J. Physiol.* **137**, 338–354.

BOYCOTT, B. B. & KOLB, H. (1973). The connections between bipolar cells and photoreceptors in the retina of the domestic cat. *J. comp. Neurol.* **148**, 91–114.

BOYCOTT, B. B. & WÄSSLE, H. (1974). The morphological types of ganglion cells of the domestic cat's retina. *J. Physiol.* **240**, 397–419.

BROWN, J. E. & MAJOR, D. (1966). Cat retinal ganglion cell dendritic fields. *Expl Neurol.* **15**, 70–78.

CLELAND, B. G. & LEVICK, W. R. (1974). Brisk and sluggish concentrically organized ganglion cells in the cat's retina. *J. Physiol.* **240**, 421–456.

CREUTZFELDT, O. D., SAKMANN, B., SCHEICH, H. & KORN, A. (1970). Sensitivity distribution and spatial summation within receptive field center of retinal on-center ganglion cells and transfer function of the retina. *J. Neurophysiol.* **33**, 654–671.

DOWLING, J. E. & BOYCOTT, B. B. (1966). Organization of the primate retina: electron microscopy. *Proc. R. Soc.* B **166**, 80–111.

FAMIGLIETTI JR, E. V. (1981). Functional architecture of cone bipolar cells in mammalian retina. *Vision Res.* **21**, 1559–1563.

FAMIGLIETTI JR, E. V. & KOLB, H. (1976). Structural basis for on- and off-center responses in retinal ganglion cells. *Science, N.Y.* **194**, 193–195.

GALLEGO, A. (1965). Connexions transversales au niveau des couches plexiformes de la rétine. *Actual. neurophysiol.* **6**, pp. 5–27. Paris: Masson et Cie.

HAMMOND, P. (1978). Inadequacy of nitrous oxide/oxygen mixtures for maintaining anaesthesia in cats: satisfactory alternatives. *Pain* **5**, 143–151.

HARTLINE, H. K. (1938). The response of single optic nerve fibers of the vertebrate eye to illumination of the retina. *Am. J. Physiol.* **121**, 400–415.

KOCH, C., POGGIO, T. & TORRE, V. (1982). Retinal ganglion cells: a functional interpretation of dendritic morphology. *Phil. Trans. R. Soc. B* **298**, 227–264.

KOLB, H. (1979). The inner plexiform layer in the retina of the cat: electron microscopic observations. *J. Neurocytol.* **8**, 295–329.

KOLB, H., NELSON, R. & MARIANI, A. (1981). Amacrine cells, bipolar cells and ganglion cells of the cat retina: a golgi study. *Vision Res.* **21**, 1081–1114.

KUFFLER, S. W. (1953). Discharge patterns and functional organization of mammalian retina. *J. Neurophysiol.* **16**, 37–68.

LEICESTER, J. & STONE, J. (1967). Ganglion, amacrine and horizontal cells of the cat's retina. *Vision Res.* **7**, 695–705.

LEVICK, W. R. (1975). Form and function of cat retinal ganglion cells. *Nature, Lond.* **254**, 659–662.

NELSON, R. (1977). Cat cones have rod input: a comparison of the response properties of cones and horizontal cell bodies in the retina of the cat. *J. comp. Neurol.* **172**, 109–136.

NELSON, R., KOLB, H., FAMIGLIETTI, JR, E. V. & GOURAS, P. (1976). Neural responses in the rod and cone systems of the cat retina: intracellular records and Procion stains. *Invest. Ophthalmol.* **15**, 946–953.

NELSON, R., FAMIGLIETTI, JR, E. V. & KOLB, H. (1978). Intracellular staining reveals different levels of stratification for on- and off-center ganglion cells in the cat retina. *J. Neurophysiol.* **41**, 472–483.

PEICHL, L. & WÄSSLE, H. (1979). Size, scatter and coverage of ganglion cell receptive field centres in the cat retina. *J. Physiol.* **291**, 117–141.

PEICHL, L. & WÄSSLE, H. (1981). Morphological identification of on- and off-centre brisk transient (Y) cells in the cat retina. *Proc. R. Soc.* B **212**, 139–156.

ROBSON, J. G. & ENROTH-CUGELL, C. (1978). Light distribution in the cat's retinal image. *Vision Res.* **18**, 159–173.

RODIECK, R. W. & STONE, J. (1965). Analysis of receptive fields of cat retinal ganglion cells. *J. Neurophysiol.* **28**, 833–849.

SCHULTZE, M. (1866). Zur Anatomie und Physiologie der Retina. *Arch. mikrosk. Anat. EntwMech.* **2**, 175–286.

STERLING, P. (1983). Microcircuitry of the cat retina. *A. Rev. Neurosci.* **6**, 149–185.

STEVENS, J. K., MCGUIRE, B. A. & STERLING, P. (1980). Toward a functional architecture of the retina: serial reconstruction of adjacent ganglion cells. *Science, N.Y.* **207**, 317–319.

WÄSSLE, H., PEICHL, L. & BOYCOTT, B. B. (1981). Morphology and topography of on- and off-alpha cells in the cat retina. *Proc. R. Soc.* B **212**, 157–175.

EXPLANATION OF PLATE

Identification of brisk transient (Y) cells from reduced silver-stained retinal whole mounts. *A*, fundus photograph of the cat eye taken after recording from an off-centre brisk transient (Y) cell. The micro-electrode is out of focus and blurred by shadows, but its tip is clearly defined. The blood vessels and their branches are well resolved. This is in the tapetal region of the fundus and the numerous dark dots are the so-called stars of Winslow (radially running choroidal capillaries). The area marked by the frame corresponds to the part taken for *B–D*. *B*, screen protocol after recording from the off- and a nearby on-brisk transient (Y) cell. The continuous outlines show the receptive field centre plot, the dotted lines indicate the back-projected blood vessels. The two asterisks mark the back-projected electrode positions from which the cells were recorded. *C*, low-power micrograph of the reduced silver-stained whole mount. The large somata are those of α cells; on many of them an axon can be resolved. Many axon bundles arch diagonally to the lower left corner. The numerous small cell bodies are those of the other ganglion cell classes. The broad, slightly curved vertical line is the major blood vessel of that area. *D*, drawing of all α-cell bodies found in *C*, classified as belonging to the on- (open profiles) or off- (filled profiles) population. The blood vessels are also drawn and the recording sites transferred from *B*. The dendritic trees are drawn for the two cells which match the recorded brisk transient units of *B*. The eccentricity of the recording area was 3 mm. *B–D* are on the same scale.

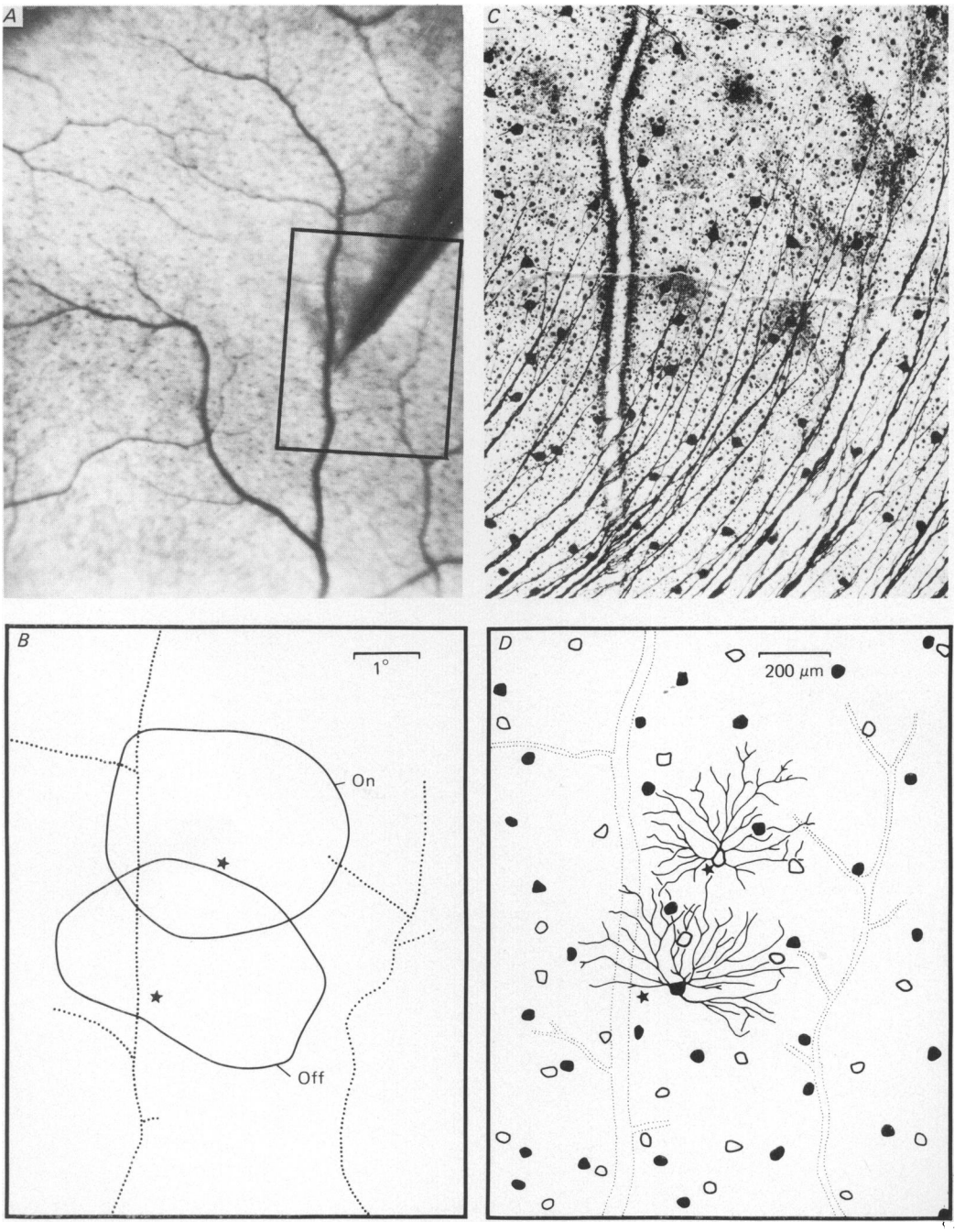
A
C
B
1°
On
Off
D
200 μm